Molecular Weight Distributions of Polydisperse Systems: Application to Very Low Density Lipoproteins†

Steven T. Kunitake, Eugene Loh, Verne N. Schumaker,* Shun Kin Ma, Charles M. Knobler, John P. Kane, and Robert L. Hamilton

ABSTRACT: A technique is described which directly yields a distribution of molecular weights. A density gradient is constructed in a centrifuge tube. Then, 0.5 mL of a dilute solution of very low density lipoproteins in a dense solvent is introduced beneath the gradient. The tube is then centrifuged until the largest lipoproteins have just floated to the top and the rest are located along the length of the tube according to their flotation coefficients. The tube is then carefully removed, mounted in a support, and scanned with an argon-ion laser. The intensity of the light scattered is proportional to the product of the concentration and the molecular weight of the lipoproteins located at each point along the tube. From their location in the tube and the conditions of centrifugation, it is possible to calculate the flotation coefficient of lipoproteins at every level. At the same time, their diffusion coefficients can be derived from the intensity fluctuations of the scattered laser light. The buoyant molecular weights can therefore be obtained at every level by combining the flotation and diffusion coefficients. By repeating the experiment in a gradient of considerably different average density, it is possible to combine the data from both experiments to obtain the molecular weights and buoyant densities at every position along each gradient. The light-scattering intensities may be divided by molecular weights to yield the concentrations at every level. All the data are then available for the construction of the distribution of molecular weights, buoyant densities, and frictional coefficients for the lipoproteins in the polydisperse sample.

Zone sedimentation velocity of macromolecules through a supporting density gradient (Schumaker, 1967), a technique originally introduced by Brakke (1960) for the study of plant viruses, was applied by Martin and Ames (1961) to study proteins, by Britton and Roberts (1960) to study ribosomes, and by Hershey (1963) to study DNA. It is an especially powerful technique for the separation and characterization of macromolecules according to differences in their sedimentation velocities. The technique may be applied on either an analytical or preparative scale. An extensive bibliography is available (Ultracentrifuge Applications, DS-463-A, Beckman, Palo Alto, Calif.).

Intensity-fluctuation spectroscopy was originally introduced by Dubin et al. (1967) as a practical technique for the study of biological macromolecules. It has provided the physical biochemist with a new and valuable tool for the determination of translational diffusion coefficients of macromolecules in small volumes of solutions. Relatively simple expositions of the theory and practical aspects of intensity-fluctuation spectroscopy have been published (Cummins et al., 1969; Fujime, 1972; Ford, 1972; Rimai et al., 1970; Pusey et al., 1974) as well as more rigorous theoretical treatments (Komarov and Fisher, 1963; Pecora, 1964, 1965).

Since the sedimentation coefficient may be divided by the diffusion coefficient to yield the buoyant molecular weight, it seems an obvious extension to combine these two techniques to yield a third, which we may call "laser scattering from centrifuged solutions". The first investigator to employ this technique, we believe, was D. E. Koppel, who illustrated its use in a study of bacterial ribosomes (Koppel, 1973). A second group of investigators (Lowenstein and Birnboim, 1975) have shown that the technique may be successfully employed using samples centrifuged in capillary tubes. They studied R17 bacteriophage and 28S rat liver ribosomal RNA.

Several aspects of the laser scattering of centrifuged solutions which we described in this communication appear to be novel: (i) A theory is presented for this new technique to yield a unique distribution of molecular weights, without having to assume shape factors or densities, for a polydisperse, macromolecular system. (ii) Experiments are analyzed using the theory to calculate the molecular weight distribution for a sample of very low density lipoproteins (VLDL). (iii) The densities and frictional coefficients of the lipoproteins are also obtained uniquely. From these results the molecular radius distribution is calculated. This radius distribution is compared with the radius distribution determined by direct measurements of particle size using the electron microscope.

Materials and Methods

Preparation of Serum Lipoproteins. Blood was drawn from a patient with mixed lipemia after a 16-h fast. EDTA[1] (0.001 M) was added to the serum to retard hydroperoxidation of olefinic lipids. A combination of antimicrobial agents was also added to the serum (sodium azide, 0.2 μg/mL; gentamycin, 5 μg/mL; and unesterified chloramphenicol, 10 μg/mL final concentration). The same concentrations of EDTA and antimicrobial agents were also present in the solutions employed in preparative ultracentrifugation and gel permeation chromatography.

The serum was ultracentrifuged for 24 h at 40 000 rpm in the 40.3 rotor in a Beckman Model L 3-50 ultracentrifuge at 12 °C. The $d < 1.006$ fraction was removed by means of a tube

† From the Department of Chemistry (Contribution No. 3812) and the Molecular Biology Institute, University of California, Los Angeles, California 90024 (V.N.S., S.T.K., E.L., C.M.K., and S.K.M.), and The Cardiovascular Institute, University of California, San Francisco, California (J.P.K. and R.L.H.). *Received July 27, 1977; revised manuscript received February 2, 1978.* This work was supported by Research Grants HL16889, HL14237, and GM13914 from the National Institutes of Health.

[1] Abbreviation used: EDTA, (ethylenedinitrilo)tetraacetic acid.

0006-2960/78/0417-1936$01.00/0

slicing device. This fraction was applied to a 2.5 × 100 cm column of 2% agarose gel as described by Sata et al. (1972) and eluted over a period of 12 h with a 0.15 M NaCl solution. Samples of lipoproteins were taken from four narrow intervals in the elution sequence so as to provide a series of fractions of lipoprotein particles of progressively smaller mean diameters.

Construction of the Density Gradient and Centrifugation of the Lipoproteins. A density gradient was first constructed in a 0.5 in. × 6 in. Corex centrifuge tube, using a commercial gradient forming engine (Beckman). The machine employed a motor-driven cam to operate six syringes which discharged into three mixing chambers, allowing the simultaneous formation of three gradients. Linear NaBr gradients were generated covering the density range 1.100–1.125 and 1.250–1.275 g/mL. One-half milliliter of the lipoprotein preparation, adjusted to a density of 1.150 or 1.300 g/mL with a saturated NaBr solution was then carefully introduced at the bottom of the centrifuge tube using a syringe and long needle. A reference sample consisting of a mixture of 3260- and of 5000-Å diameter polystyrene latex spheres was prepared for centrifugation in the same rotor. The polystyrene density was 1.055 g/cm^3 and its concentration was approximately 100 μg/mL. A sucrose gradient which ranged in density from 1.010 to 1.035 g/mL was used for the reference tube. The sucrose solution also contained 0.01 M NaCl and 0.01% Triton X-100. A 0.2 mL volume of polystyrene solution in 0.01 M NaCl and 0.01% Triton X-100 was layered on top of the sucrose gradient. Two sharp, sedimenting zones were observed for the reference sample, corresponding to the locations of the 3260- and 5000-Å particles.

Centrifugation. The gradient tubes were carefully transferred to a Sorvall Type HB4 swinging-bucket rotor mounted in an RC5 centrifuge. The centrifuge was modified by the introduction of a rate controller, obtained from the manufacturer, which permitted gradual acceleration and deceleration of the rotor to minimize gradient disturbance. The samples were centrifuged for 20 min at 10 000 rpm (1.100–1.126 g/mL gradients) or 20 min at 7000 rpm (1.250–1.275 g/mL). Centrifugation was at room temperature. There were no detectable disturbances caused by handling of the tubes before and after centrifugation.

Laser Scattering from Centrifuged Samples. A 2-W argon-ion laser (Spectra Physics, Model 165) was used in these studies. The top of the centrifuged gradient tube was inserted into a plastic holder mounted on the end of a depth micrometer with a 2-in. vertical traverse. The micrometer assembly was supported on a stand and the tube accurately centered in the laser beam before the micrometer assembly was clamped in place. The scattered laser light was focused on an EMI 9558B photomultiplier (Whittaker, Plainview, N.Y.), and the DC signal generated, which is proportional to the intensity of the scattered light, was directly read with a digital voltmeter (Model 190 Multimeter, Keithley, Cleveland, Ohio). A schematic drawing of this apparatus is shown as Figure 1. The AC signal was sent to a Saicor (Honeywell, Denver) 43A autocorrelator for the accumulation of the autocorrelation function. The output of the autocorrelator was first transferred to a PDP-8 and then to a PDP-11/45 computer for data analysis and plotting. The intensity scattered at a given angle was scanned along the length of the tube and recorded on a strip chart recorder; the correlation function was measured at seven heights. Diffusion measurements at each position required 5 to 10 min, depending upon scattered intensity. The temperature of the sample was measured by a calibrated thermistor (VECO 32A14, Victory, Springfield, N.J.) taped on the outside of the sample tube, which had been verified to have the same temperature as the solution inside.

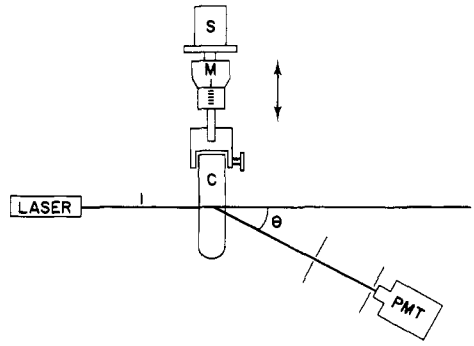

FIGURE 1: Schematic representation of laser scattering apparatus. The centrifuged tube (C) is suspended from a vertical transverse micrometer (M) driven by a stepping motor (S) which allows the tube to move in a direction perpendicular to the incoming laser beam (I). A photomultiplier tube (PMT) can then receive the scattered signal at any angle, θ, in a plane perpendicular to the axis of the tube.

Calibration of Gradients, Centrifugation Conditions, and Scattered Intensities. The linearity of the density gradients generated along the length of centrifuge tubes was checked by refractive index measurements. The tube contents were first fractionated into 0.40-mL portions with an ISCO (Lincoln, Neb.) density gradient fractionator. Fractions were removed from the top by pumping a high-density fluorocarbon (Fluorinert, 3M Company, St. Paul, Minn.) into the bottom of the tube to displace the gradient. The refractive index of each fraction was determined with an Abbé refractometer (Bausch and Lomb).

In order to calibrate the conditions of centrifugation, a number of centrifuge runs were made with the polystyrene samples in sucrose–0.01 M NaCl gradients. Particle positions were measured using the laser-scattering apparatus. Temperatures were measured before and after each centrifuge run in a reference centrifuge tube. The values of the $\omega^2 t$ integral were calculated from the expression:

$$\int_0^t \frac{\eta_{20,w}}{\eta_{T,w}} \omega^2 dt = \frac{1}{s_{20,w}} \int_{r_0}^{r} \frac{\eta_{T,s}}{\eta_{T,w}} \frac{(1 - \phi\rho_{20,w})}{(1 - \phi\rho_{T,s})} d \ln r \quad (1)$$

where r is radial position along the tube axis and r_0 is the initial position of the polystyrene zone, η and ρ are solvent viscosity and density, ϕ is the apparent specific volume of the polystyrene, taken as 0.948 mL/g, $s_{20,w}$ is the polystyrene sedimentation coefficient corrected to water at 20 °C, t is time, and ω is angular velocity. A good correlation between the values of the integral:

$$\int_0^t \frac{\eta_{20,w}}{\eta_{T,w}} \omega^2 dt$$

calculated from the sedimentation properties of the 0.500- and the 0.326-μm diameter polystyrene particles is shown in Figure 2.

Electron Microscopy. The special technical procedures of grid preparation and negative staining were described in detail in a previous report (Hamilton et al., 1971). Samples were photographed at 20 000 diameters at 80 kV in a Siemens 101 electron microscope with a condenser aperature of 200 μm and an objective aperature of 60 μm. Particle diameters were measured directly on negatives using an optical microcomparator (Nikon Model 6C, Nippon Kogaku, Tokyo, Japan).

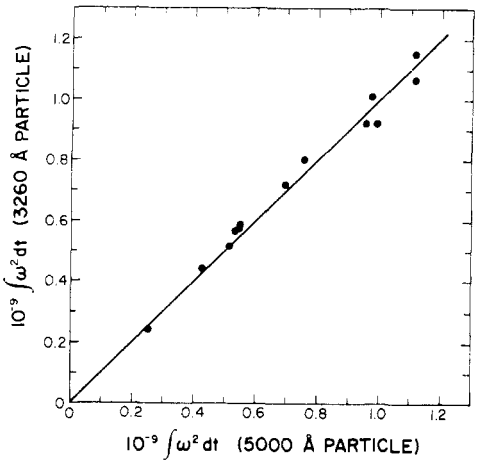

FIGURE 2: Time and rotor speed calibration. To demonstrate internal consistency and precision, values of the "ω^2dt" integral obtained for the 0.500- and 0.326-μm particles centrifuged together in the same gradient are plotted against each other. The solid line has a slope of 1.

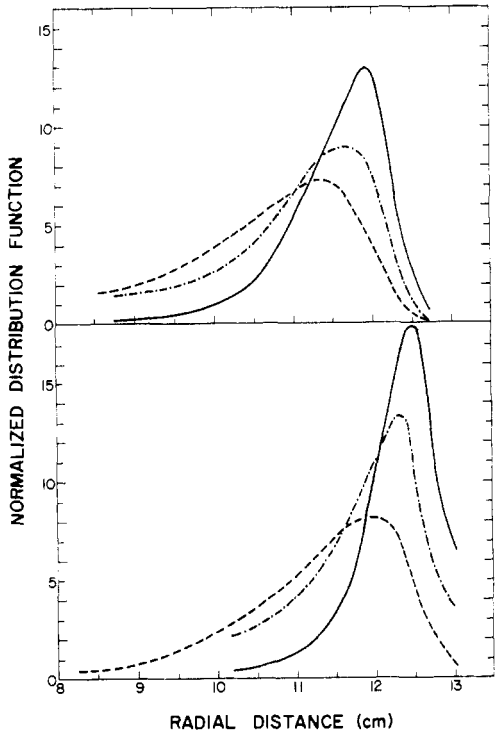

FIGURE 3: Normalized distribution functions of lipoproteins as related to the radial distance in the centrifuge tube for the medium gradient (A, top) and the heavy gradient (B, bottom): (- - -) the direct scattering intensity distribution; (- • -) normalized weight concentration distribution corrected for particle scattering factor and differences in scattering power due to differences in index of refraction with location in the gradient; (—) number concentration of lipoprotein particles along the centrifuge tube. All distributions were normalized to give equivalent areas beneath the curves.

All samples were photographed the same day of the grid preparation. A variety of manipulations were used to obtain uniform spreading of particles on the grid surface before a sample was photographed for sizing. These included increasing the contact time of the sample on the grid surface for more dilute samples, using grids of different mesh, and, importantly, using grids that were aged on the bench from 6 to 12 months. Aging appears to reduce the hydrophobicity or increase the wettability of the grid surface, thereby greatly reducing "snow" artifacts commonly encountered in negative stains of samples

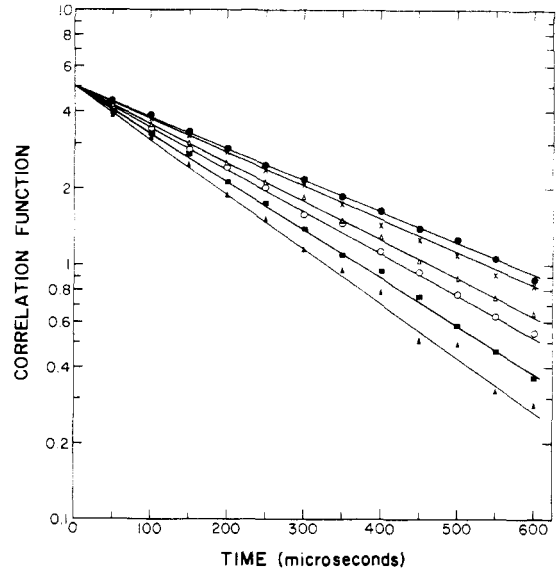

FIGURE 4: Intensity-fluctuation spectroscopy. A semilog plot of several correlation functions as a function of time. The diffusion coefficient is inversely proportional to the slope of each line. Each line represents a spectrum taken at a different position along the centrifuge tube. The steepening of the slopes indicates that as the radial distance increases smaller particles are found.

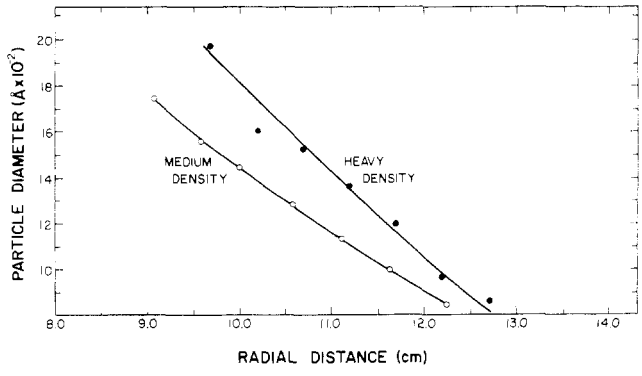

FIGURE 5: A plot of apparent particle diameter as a function of radial position in the centrifuge tube. The diameters were obtained from the diffusion measurements shown in Figure 4, using Stokes' law. This plot was used to determine the radial location of particles having the same diameter in the medium- and heavy-density gradients.

containing nonpolar constituents. Finally, aggregation of particles is avoided by staining the lipoproteins on the wet grid surface (Hamilton et al., 1971) rather than mixing the lipoproteins and phosphotungstate before applying the mixture to the grid as is commonly practiced.

Results

Light Scattering from Centrifuged Samples of VLDL. One-half milliliter samples of the lipoprotein preparations were centrifuged in the 1.100–1.125 (medium density) and the 1.250–1.275 g/mL (heavy density) gradients. The results are shown in Figure 3 for the first fraction from the agarose column. The highly polydisperse lipoprotein sample occupies approximately two-thirds the length of the centrifuge tube, as may be seen from the distributions of light-scattering intensities.

The diffusion coefficients of the lipoproteins were determined at selected locations along the tube. These are shown in Figures 4 and 5. Figure 4 shows the decay of the autocorrelation function. The diffusion coefficient is derived from the initial slope. Figure 5 is a plot of these diffusion data for the

TABLE I: Hydrodynamic Parameters for Very Low Density Lipoproteins.

Radius[a] (Å)	$D_{20,w}$[b] (ficks)	$F_{20,1.11}$[c] (S)	ϕ[d] (mL/g)	M[e] ($\times 10^6$ daltons)	f/f_0[f]	ϕ_{calcd}[g] (mL/g)
424.9	0.5052	649	1.056	181.8	1.000	1.054
501.5	0.4281	983	1.064	309.0	0.987	1.063
566.5	0.3789	1275	1.070	436.9	0.992	1.066
641	0.3348	1581	1.072	605.9	1.006	1.069
720	0.2981	1976	1.080	812.5	1.022	1.072
780	0.2753	2260	1.085	979.0	1.038	1.073
869.5	0.2469	2613	1.080	1297.3	1.055	1.075

[a] Stokes' radius as determined from $D_{20,w}$ (Figure 3, bottom). [b] Data from Figure 3 (bottom), medium-density gradient. [c] Flotation coefficients corrected to standard conditions, which for these studies were conveniently selected as a hypothetical solvent with the viscosity of water but with a density of 1.11 g/mL. [d] Apparent specific volume as determined from the intersection points shown in Figure 4. [e] Lipoprotein molecular weight, calculated from eq 5. [f] Lipoprotein frictional ratio, calculated from eq 6. [g] Calculated apparent specific volume for a lipoprotein with the given outer radius, composed of a core with a density of 0.915 g/mL surrounded by a shell with a density of 1.10 g/mL and a thickness of 22.5 Å.

medium- and heavy-density gradients, presented as Stoke's radii $R = kT/6\pi\eta D$ where k is the Boltzmann constant, T is the temperature during measurement, η is the viscosity in the gradient at the position of measurement, and D is the observed diffusion coefficient.

The data presented in Figure 5 permit the comparison of the lipoprotein distributions in the medium- and heavy-density gradients. They enable us to mark the location of the same lipoproteins in the two different gradient tubes. Thus, a lipoprotein possessing a given Stoke's radius may be selected on the vertical axis of Figure 5. Then, using the two curves, the corresponding positions of these lipoproteins in two different gradients may be read directly from the horizontal axis. This ability to locate the same lipoproteins in the two different gradient tubes is the key to the analysis that is to follow.

Determination of Flotation Coefficients and Apparent Specific Volumes of the Lipoprotein Particles. Mathematically it is most convenient to select a standard flotation coefficient close to the value determined in one of the two gradients employed in these studies. Arbitrarily, we have selected as a standard state the flotation coefficient $F_{20,1.11}$, which is defined in terms of the experimentally measured (negative) sedimentation coefficient:

$$F_{20,1.11} \equiv -\frac{(1 - \phi_{20,1.11} \times 1.11)}{(1 - \phi_{T,s} \times \rho_{T,s})} \frac{\eta_{20,s}}{\eta_{20,w}} s_{T,s} \qquad (2)$$

Therefore, the standard flotation coefficient that we calculate is a hypothetical value in a hypothetical solvent of density of 1.11 g/mL, but with the viscosity of water at 20 °C.

An equation corresponding to eq 1 then may be written for the lipoproteins:

$$\int_0^t \frac{\eta_{20,w}}{\eta_{T,w}} \omega^2 dt = -\frac{1}{F_{20,1.11}} \int_{r_0}^{r} \frac{\eta_{T,s}}{\eta_{T,w}} \frac{(1 - \phi_{20,1.11} \times 1.11)}{(1 - \phi_{T,s} \times \rho_{T,s})} d \ln r \qquad (3)$$

In using eq 3 it is convenient to assume that $\phi_{T,s} = \phi_{T,1.11} = \phi$. That is, we will assume that the buoyant specific volume does not change significantly with salt concentration in the range over which we are working. This assumption will be discussed critically in the last section of this paper.

Inspection of eq 3 shows that it contains two unknown quantities, $F_{20,1.11}$ and ϕ. Everything else may be measured or calculated. Thus, the integral on the right-hand side of eq 3 may be computed by the following procedure for a lipoprotein particle that has moved from r_0 to r. First, the functional relationships between the viscosity and radial position and the density and radial position were determined. To do this, the viscosity and density of sodium bromide solutions were expressed in power series in refractive index, using values of $\tilde{n}$ taken from the International Critical Tables:

$$\frac{\eta_{T,s}}{\eta_{T,w}} = A + B(\tilde{n} - \tilde{n}_0) + C(\tilde{n} - \tilde{n}_0)^2 \qquad (4a)$$

$$\rho_{T,s} = D + E(\tilde{n} - \tilde{n}_0) + F(\tilde{n} - \tilde{n}_0)^2 \qquad (4b)$$

For sodium bromide gradients in the density range between 1.10 and 1.125 g/mL, we used $A = 1.075$, $B = 5.3135$, $C = 195.3125$, $D = 1.0981$, $E = 5.640625$, and $F = 24.4141$. For the density range between 1.25 and 1.30 g/mL, we used $A = 1.172$, $B = 8.79863$, $C = 171.625$, $D = 1.2163$, $E = 5.95614$, and $F = 0$. Since the variation of refractive index with radial distance is known, eq 4a and 4b can be used to determine the values of relative viscosity and density at every point, r, within the centrifuge tube.

All the quantities required for the calculation of the integral on the right of eq 3 are now known except for the ϕ's, the buoyant specific volumes of the lipoproteins. Therefore, we selected a set of ϕ values that should lie in the range of values expected to be found for the VLDL lipoproteins. Since these lipoproteins have buoyant densities ($= \phi^{-1}$) ranging between 0.90 and 1.00 g/mL, we selected test values of 0.90, 0.92, 0.94, 0.96, 0.98, and 1.00 g/mL. Then, using each test value of ϕ in turn, the integral (eq 3) was solved at 40 different r values along the length of the centrifuge tube. This was done by computer, and the entire set of numbers was tabulated. Thus, for any given value of ϕ and r, the corresponding value of the integral on the right-hand-side of eq 3 could be read directly or interpolated from the table. Separate tables were prepared for the medium and heavy gradients.

In order to determine the two unknown quantities F and ϕ for a given lipoprotein species, data were collected in two separate centrifuge experiments using the medium- and heavy-density gradients. A separate eq 3 can be written for each lipoprotein species in each gradient, and the pair of equations can be solved simultaneously. Although the same lipoprotein species are located at different r values in the different gradients, they could be identified by their characteristic $D_{20,w}$ values. This location procedure was described for Figure 5. The solution of each pair of simultaneous equations is then performed graphically, as shown in Figure 6. Values of $F_{20,1.11}$ are plotted as a function of ϕ for both the medium- and

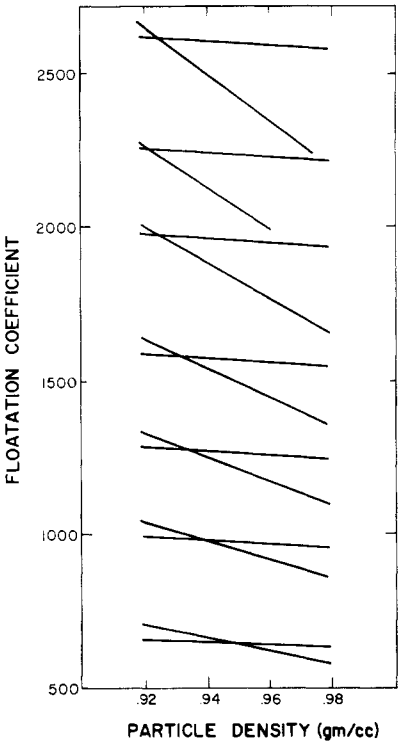

FIGURE 6: Flotation coefficient vs. particle density for seven different particle diameters. The lines were obtained by plotting $F_{20,1.11}$ as a function of ϕ^{-1} using eq 3 for both the heavy- and medium-density gradients. The points of intersection uniquely define $F_{20,1.11}$ and ϕ^{-1} for the seven different particle diameters.

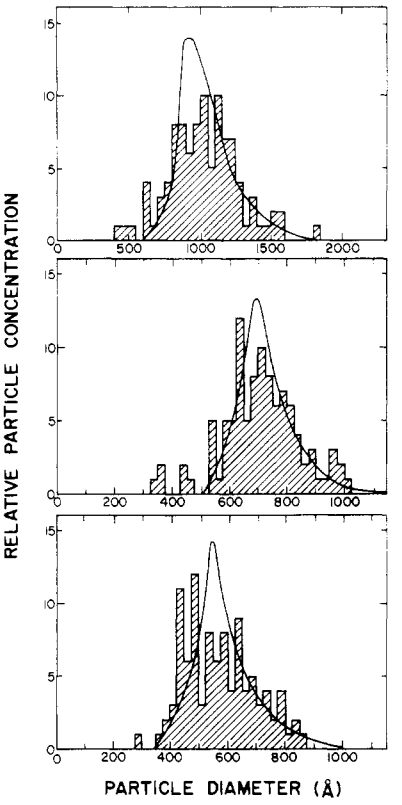

FIGURE 7: Particle distributions. Plots of number-average particle concentration vs. particle diameter. The histograms represent data obtained from measuring 100 particles with the electron microscope. The solid curves are the distributions obtained by laser scattering. For the purposes of comparison, the area beneath the curve was made equal to the shaded area of the histogram. (A, top) Sample SF-16, from which the data shown in Figures 2–5 were obtained. The mean diameter obtained from the electron microscope histogram is 1030 Å and the standard deviation is 249 Å. The corresponding values obtained by the light-scattering technique are 1054 ± 190 Å. (B, middle) Sample SF-22. For the EM distribution, the mean and standard deviations are 708 ± 231. By light scattering these values are 730 ± 95 Å. (C, bottom) Sample SF-29. For the EM distribution, the mean and standard deviations are 574 ± 122 Å. For light scattering, these values are 590 ± 106 Å.

heavy-density gradients. The intersection of the two curves provides a unique solution and yields the values of ϕ and F for the corresponding lipoprotein species. For our experiments, these values are listed in Table I.

Determination of Molecular Weights and Frictional Ratios. Molecular weights were computed from the Svedberg equation:

$$M_i = \frac{-F_i \mathcal{R} T}{D_i(1 - \phi_i \times 1.11)} \tag{5}$$

where the subscript i stands for each lipoprotein species in turn. The values of $F_{20,1.11}$ and $D_{20,w}$ are those for standard solvent conditions, T = 20 °C, ρ = 1.11 g/mL, and $\eta_{20,w}$ = 0.9982 cP.

The translational frictional ratio has been computed from the flotation equation:

$$(f/f_0)_i = \frac{-M_i^{2/3}(1 - \phi_i \times 1.11)}{F_i N 6\pi\eta_{20,w}(3\phi_i/4\pi N)^{1/3}} \tag{6}$$

Values for M_i and $(f/f_0)_i$ are listed in Table I.

Determination of the Distribution of Particle Diameters. The distributions of lipoproteins, shown as the dashed curves in Figure 3, are actually distributions of light-scattering intensities. Light scattering intensity is proportional to the product of weight concentration and molecular weight. Therefore, to determine a number proportional to the weight concentration of the lipoprotein particles at each point along the tube, it is necessary to divide by the corresponding molecular weight.

Actually, the correction is a bit more complicated than this, for one should also take into account the variation in refractive index increment of the lipoproteins with solvent composition along the length of the gradient. Moreover, a particle-scattering factor correction must be applied, for these lipoproteins have diameters that are appreciable compared with the wavelength of light (Tanford, 1961, eq 18-1, 18-17, and 18-20). Large particle size causes the scattering intensities to decrease by 14% for a particle that is 750 Å in diameter and 38% for a particle that is 1250 Å in diameter.

When all corrections have been applied, the distribution of weight concentrations is obtained, as shown by the dash-dot line in Figure 3.

In order to compare our results with those obtained by electron microscopy, however, it is necessary to calculate the number distribution of the lipoprotein particles. Once again, we must divide by the molecular weight. In Figure 3, the number distribution is shown as the solid line.

The electron microscope distributions are shown as histograms in Figure 7. The horizontal axes are particle size. In order to change the number distribution of Figure 3 (top) into the number distribution shown in Figure 7 (top), it is necessary to transform both the ordinate and abscissa values. If R is the particle radius and r is the length along the centrifuge tube, then we convert between these quantities using the expression:

$$\ln(r/r_0) = \frac{2}{9}\frac{R^2(1 - \phi\rho)}{\phi\eta}\omega^2 t \tag{7}$$

To transform the ordinate values of dn/dr, where n is the

number of particles, into the radial distribution, dn/dR, we use the transformation:

$$\frac{dn}{dR} = \left(\frac{dn}{dr}\right)\left(\frac{dr}{dR}\right) \quad (8)$$

The partial derivative is evaluated from eq 7. For this purpose, we assumed that $(1 - \phi\rho)/\phi$ is constant, as it makes little difference in the final result. Therefore,

$$\frac{dn}{dR} = KrR\left(\frac{dn}{dr}\right) \quad (9)$$

where K is a normalization constant to yield the same area beneath the smooth curve as is contained within the histogram.

Discussion

In order to interpret the hydrodynamic data obtained with this technique in terms of molecular weights, frictional ratios, and apparent specific volumes, it is necessary to make two implicit assumptions. The first of these is that the measurement of the diffusion coefficient uniquely identifies a single species of macromolecule that can be located at a distinct position in each of the two gradients. The analysis would break down if the mixture contained particles of different molecular weights, densities, etc., which appeared at the same location in one of the gradients but at two separate places in the other.

In the studies reported in this communication, this first assumption is probably valid. Thus, a nearly homologous series of VLDL was seen with the electron microscope. These were particles that appeared to be spherical in shape and differed only in particle size. No unusually large or membranous structures were seen in these preparations.

The second assumption required in order to solve eq 3 is that the apparent specific volume of a lipoprotein species does not change with sodium bromide concentration. Indeed, for the analysis to be strictly valid, ϕ must remain constant for a given lipoprotein as the solvent density changes from 1.10 to 1.30 g/mL. Only a little data are available for serum lipoproteins, and even that is for the LDL species and not for the VLDL lipoproteins that have been studied here. For the LDL, however, the ηs vs. ρ plots are straight over the range between 1.00 and 1.20 g/mL for a KBr solvent (Fisher et al., 1971). This would imply that ϕ is constant for LDL.

For VLDL, the variation in ϕ must be relatively small because reasonable values of this quantity are found in our experiments. We may compare the experimentally determined values with those obtained from a reasonable model for VLDL. In this model the lipoprotein is represented by a central core of triglyceride of density 0.915 g/mL and a shell of phospholipid and protein 22.5-Å thick with an average density of 1.10 g/mL (Sata et al., 1972). The values for the apparent densities (ϕ^{-1}) calculated from this model are listed in Table I for comparison with the values determined by experiment. The experimental densities tend to be a little lower, but the trend is the same.

Most of the frictional ratios listed in Table I seem surprisingly close to 1.00. The reproducibility of our measurements of f/f_0 is fair; thus, the average value of the frictional ratios listed in Table I is 1.014 ± 0.023, and for the data described in Figure 7 (center and bottom) the average values of f/f_0 are 1.049 ± 0.034 and 1.012 ± 0.069, respectively. Since we are using the experimentally determined buoyant specific volumes in our calculations, values of f/f_0 close to 1.00 would imply that the hydrodynamic unit is spherical and that the density of the hydration layer does not change with salt concentration. It is of interest to calculate the frictional ratio and buoyant specific volume which would be found by application of our technique if the lipoproteins actually bound a thick layer of ambient density solvent. Thus, for a spherical lipoprotein with a radius of 500 Å and a buoyant specific volume of 1.063 mL/g which binds a shell of ambient solvent 10-Å thick, we would find by our technique values of 1.020 and 1.063 mL/g for f/f_0 and ϕ, respectively. These values would lie within the precision of our measurements. Or we might assume that this lipoprotein bound a 10-Å shell of ambient solvent in the medium-density gradient but was completely dehydrated in the heavy gradient. Since we compare particles with equal Stokes radii in the two gradients, we select an unhydrated particle with a diameter of 510 Å in the heavy gradient. If the data were to be analyzed as before, then values of 0.977 and 1.0386 mL/g would be found for the frictional ratio and buoyant specific volume. The value for the frictional ratio would lie within the precision of our measurements. However, the value for the buoyant specific volume would be significantly lower than the value of 1.063 g/mL calculated from lipid composition (Table I). Thus, we are forced to conclude that even fairly substantial amounts of hydration might go undetected. There are three reasons for this: (1) we are using measured buoyant specific volumes, (2) we are comparing particles with the same Stokes' radii, and (3) these lipoproteins are very large particles with an apolar interior which probably sharply limits the interpenetration of water and salt to a shell a few angstroms thick at the surface. Even a 10-Å shell would only increase the frictional ratio by 2% for a 500-Å particle, while for a 50-Å globular protein a shell of the same thickness would give a value of 1.20 for f/f_0.

The agreement between the values for the distribution of particle radii found by the laser scattering technique and by electron microscopy is gratifying (Figure 7). Thus, the particles could not be much flattened on the electron microscope grid, nor could they be greatly swollen in solution.

We believe the technique presented here, and the method of analysis, may find wide application for the measurement of particle size, shape, and density distributions for a wide variety of large particles, including lipoproteins, membrane vesicles, and virus particles. It is possible that small cell organelles also may be profitably studied by this new technique of laser scattering from centrifuged solutions.

References

Britton, R. J., and Roberts, R. B. (1960), *Science 131,* 32.

Camerini-Otero, R. D., Pusey, P. N., Koppel, D. E., Schaefer, D. W., and Franklin, R. M. (1974), *Biochemistry 13,* 960.

Cheng, P. Y., and Schachman, H. K. (1955), *J. Polymer Science, 16,* 19.

Cummins, H. Z., Carlson, F. D., Herbert, T. J., and Woods, G. (1969), *Biophys. J. 9,* 518.

Dubin, S. G., Lunacek, J. H., and Benedick, G. B. (1967), *Proc. Natl. Acad. Sci. U.S.A. 57,* 1164.

Fisher, W. B., Granade, M. E., and Mauldin, J. L. (1971), *Biochemistry 10,* 1622.

Ford, N. C., Jr. (1972), *Chem. Sci. 2,* 193.

Fujime, S. (1972), *Adv. Biophys. 3,* 1.

Hamilton, R. L., Havel, R. J., Kane, J. P., Blaurock, A. E., and Sata, T. (1971), *Science 172,* 475.

Hershey, A. D., Burgi, E., and Ingraham, L. (1963), *Proc. Natl. Acad. Sci. U.S.A. 49,* 748.

Komarov, L. I., and Fisher, I. Z. (1963), *Sov. Phys. JETP (Engl. Transl.) 16,* 1358.

Koppel, D. E. (1973), Ph.D. Thesis, Columbia University, New

York, N.Y.
Lowenstein, M. A., and Birnboim, M. H. (1975), *Biopolymers 14,* 419.
Martin, R. G., and Ames, B. N. (1961), *J. Biol. Chem. 236,* 1372.
Pecora, R. (1964), *J. Chem. Phys. 40,* 1604.
Pecora, R. (1965), *J. Chem. Phys. 43,* 1562.
Pusey, R. N., Koppel, D. E., and Schaefer, D. W. (1974), *Biochemistry 13,* 952.
Rimai, L., Hickmott, J. T., Jr., Cole, T., and Carew, E. B. (1970), *Biophys. J. 10,* 20.
Sata, T., Havel, R. J., and Jones, A. L. (1972), *J. Lipid Res. 13,* 757.
Schumaker, V. N. (1967), *Adv. Biol. Med. Phys. 11,* 245.
Tanford, C. (1961), Physical Chemistry of Macromolecules, Wiley, New York, N.Y.

Chemical and Enzymatic Properties of Riboflavin Analogues†

Christopher Walsh,*,‡ Jed Fisher,§ Rob Spencer,¶ Donald W. Graham, Wallace T. Ashton, Jeannette E. Brown, Ronald D. Brown, and Edward F. Rogers*

ABSTRACT: The chemical and enzymatic properties of 26 analogues of riboflavin are presented. These analogues include both endo- and exocyclically substituted isoalloxazines with redox potentials from −370 to −128 mV. Physical and chemical data such as the electronic absorption spectra, pK_as, and redox potentials of the analogues are presented and are discussed with respect to preferred tautomeric and resonance forms. Like riboflavin, most of the analogues are shown to be catalytic oxidants of dihydro-5-deazaflavins. Analogue binding to egg white binding apoprotein has been quantitated and serves to determine the origins of binding site specificity for this protein. Nearly all of the analogues that possess D-ribityl groups are found to be processed to the FAD level by the flavokinase/FAD synthetase system of *Brevibacterium ammoniagenes.* Most extensively studied are the reactivities of the analogues with the NAD(P)H:flavin oxidoreductase of *Beneckea harveyi.* Many of the analogues are substrates in this enzymatic redox reaction, and a linear free energy–rate relation (log V_{max} vs. E_0' of the analogue) is seen that parallels similar relationships in the nonenzymatic oxidation of dihydro-5-deazaflavins. This suggests a common mechanism for the reactions of such diverse flavins as riboflavin, 5-deazariboflavin, and 1-deazariboflavin.

In the past few years there has been increasing interest in the preparation of isosteric replacements for enzyme substrates and coenzymes. Such molecules have potential both as therapeutic agents and as models with which to probe the mechanisms of enzyme catalysis (Rivlin, 1975; Singer, 1976). Several analogues of the flavin coenzymes have been shown to have antivitamin activity (Lambooy, 1975; Lambooy & Shaffner, 1977; Chu & Bardos, 1977; Otani, 1976). One class of such flavin analogues involves exocyclic substitutions (particularly at N-10) that do not alter the chemistry of the isoalloxazine ring system, so that their in vivo activity is based on steric, not chemical, changes. Another class involves isosteric substitutions that alter the coenzyme redox chemistry. In this paper we explore these two categories with a series of riboflavin analogues recently synthesized by Rogers and colleagues (Ashton et al., 1977; Graham et al., 1977). Several of these have already been shown to be potent anticoccidial agents (Graham et al., 1977).

In order to use these analogues as probes of flavin redox chemistry and, perhaps, to understand the bases of their in vivo activities, we have surveyed the elementary chemistry (pK_as, redox potentials, behavior in a redox model system reaction) of the analogues. We also present results of assays with the analogues in three in vitro flavoprotein systems: the egg white binding protein, the flavokinase and FAD synthetase from *Brevibacterium ammoniagenes,* and the NAD(P)H:flavin oxidoreductase from *Beneckea harveyi.* Much of this information is self-explanatory and is presented in Tables I and II; the observations of particular interest as well as correlations between the chemical and enzymatic properties of the analogues are presented in the Results and Discussion.

Experimental Section

Materials

The flavin analogues were prepared or purchased as follows (numbering as in Tables I and II[1]): **1,** Shunk et al. (1952); **2, 6, 12b,** Graham et al. (1977); **4, 10,** from Sigma Chemical; **5,** Shunk et al. (1955); **8,** from **10** by snake venom phosphodiesterase cleavage; **9,** Yagi (1971); **11,** Berezovskii & Rodionova, (1958); **12,** a generous gift of Dr. Shiao-Chun Tu; **13, 14, 18,** Ashton et al. (1977); **15,** O'Brien et al. (1970); **20,** Yoneda et al. (1976), with a modified preparation of the intermediate 6-(*N*-D-ribityl-3,4-xylidino)uracil (W. T. Ashton, R. D. Brown, & R. L. Tolman, submitted for publication); **21a, 21d, 21e,** from **3** and an excess of the appropriate amine by heating at 100 °C in dimethylformamide for several hours.

7,8-Didemethyl-8-chlororiboflavin (**3**) was prepared by the method of Haley & Lambooy (1954) for 8-demethyl-8-chlororiboflavin. 2,4-Dichloronitrobenzene and D-ribitylamine

† From the Departments of Chemistry and Biology, Massachusetts Institute of Technology, Cambridge, Massachusetts 02139 (C.W., J.F., and R.S.), and the Merck, Sharp, and Dohme Research Laboratories, Rahway, New Jersey 07065 (D.W.G., W.T.A., J.E.B., R.D.B., and E.F.R.). *Received August 10, 1977; revised manuscript received December 1, 1977.* Work performed at MIT was supported in part by National Institutes of Health Grant GM 21643.

‡ Alfred P. Sloan Fellow 1975-1977; Camille and Henry Dreyfus Scholar 1975-1980.
§ Current address: Department of Chemistry, Harvard University, Cambridge, Massachusetts 02138.
¶ National Science Foundation Predoctoral Fellow 1974-1977.

0006-2960/78/0417-1942$01.00/0